Hindawi
Journal of Sensors
Volume 2022, Article ID 4247277, 15 pages
https://doi.org/10.1155/2022/4247277

Research Article

Numerical Investigation on ELF Electromagnetic Field Distribution of Pipeline Robot Tracking and Positioning System Using UAV

Bao Tian,[1] **Zhaolin Yang**,[2] **Shouhong Ji**,[2] **Xiang Chen**,[3] **and Kun Zhao**[1]

[1]*School of Intelligent Engineering, Zhengzhou University of Aeronautics, Zhengzhou 450046, China*
[2]*PipeChina Zhejiang Pipeline Network Co., Ltd., Hangzhou 310052, China*
[3]*School of Intelligent Manufacturing, Huanghuai University, Zhumadian 463000, China*

Correspondence should be addressed to Bao Tian; tbswpu@163.com

Received 9 September 2022; Revised 14 November 2022; Accepted 19 November 2022; Published 19 December 2022

Academic Editor: Akhilesh Pathak

Pipeline robot, as a new type of equipment for pipeline operations such as pigging and detection, will play an increasingly important role in the operation and maintenance of oil and gas pipeline networks. The tracking and positioning technology during its operation process is one of the essential topics to improve the operating performance of pipeline robots and eliminate potential pipeline accidents. This paper presents the overall design of the wireless tracking and positioning system for pipeline robots based on extremely low frequency (ELF) electromagnetic method using the unmanned aerial vehicle (UAV). Starting from the classical electromagnetic theory, a mathematical model for the distribution of ELF electromagnetic field in buried metal pipeline environment is established. According to the characteristics of ELF electromagnetic wave transceiver and the model based on classical theory, the equivalent magnetic dipole transmission model is deduced. Based on the equivalent model, the attenuation characteristics of the ELF electromagnetic wave in the external space of the pipeline are analyzed by numerical simulation. The influence of the geometrical dimensions, environmental and working parameters, and other factors on the electromagnetic field intensity outside the pipeline is given at the same time. Finally, the distribution of ELF electromagnetic field in pipeline environment is discussed for horizontal-laying pipeline and inclined-laying pipeline, and the tracking method of pipeline robot is proposed on this basis. The proposed scheme is practical and effective, and it is suitable for real-time tracking and positioning of robot working in the pipelines whose slope is no more than 60 degrees with known or unknown distribution.

1. Introduction

As the primary way of oil and natural gas transportation, pipeline plays a vital role in industrial production and civil use. During the laying period and long-term operation, pipelines will inevitably produce dirt sedimentation, deformation, corrosion, and other hidden troubles, which not only reduce the transportation capacity and increase the production cost but also may cause oil or gas leakage and even lead to safety accidents in severe cases. Consequently, strengthening the regular cleaning, testing, and maintenance of oil and gas pipelines is of great significance to ensure the safe operation and prolong the service life of pipelines. Pipeline robot, represented by intelligent pig and internal detector, has been more and more used in the daily maintenance of pipelines due to its unique advantages and is increasingly becoming an essential application carrier in pipeline safety assurance system. However, when the pipeline robot moves in the pipeline, it may get stuck in the pipe due to the pipeline deformation, sediment accumulation, the failure of its system, etc., which may lead to pipeline blockage, affect the normal transportation of oil and gas, and even endanger the safety of pipe network [1]. Therefore, when pipeline robot performs pigging or inspection operations, technicians need to grasp its movement status and accurate position in real-time through effective tracking and positioning technology,

so as to take corresponding measures to quickly and accurately handle the accident and resume production.

With the development of pipeline robot technology, its tracking and positioning technology has experienced a process from "through instruction", "accurate positioning" to "tracking" [2, 3]. "Through instruction" means that the pipeline robot sends a specific prompt when passing through a particular position of the pipeline [4]. The typical implementation method is mechanical method, and the equipment used is passage indicator. This method has a low-operating cost, but the false alarm rate is high. It can only obtain the information of whether the robot passes through a specific position, but cannot obtain the accurate position information at its runtime. "Accurate positioning" is to determine the exact position of the robot by using equipment such as transmitters and receivers based on "through instruction" in response to accidents such as the jamming of the robot. Typical implementation methods include magnetic method, acoustic method, pressure method, and radioisotope method. The principle of the magnetic method is to install a transmitter that emits an ELF electromagnetic pulse signal on the robot, detect the pulse signal outside the tube through the receiving coil, and indicate the location of the pipeline robot after processing [5–7]. The advantage of this method is that the signal has strong penetrating power and can penetrate the soil of the pipe wall. It is suitable for many occasions, but it has higher requirements for the sensitivity, response speed, and portability of the receiving device. Acoustic-based positioning methods include noise method, acoustic wave feature discrimination method, and ultrasonic method. Its principle is to record and analyze the acoustic wave characteristics generated by the pipeline robot when it is running or to receive the pulse signal emitted by the ultrasonic transmitter installed on the robot for positioning. The disadvantage is that the signal attenuation is fast, the noise signal interference is significant, and the application range is limited [8, 9]. The pressure method is to realize positioning through different pressure values detected by two pressure transmitters when the robot passes. The pressure method can use the pressure and flow data obtained in the field to judge the operation of the robot, but the monitoring distance is relatively short, which requires high work experience for operators, and its practicability needs further research. The principle of the radioactive isotope method is to install a radioactive source on the robot and indicate the position of the robot by detecting the rays emitted by the radioactive isotope tracer [10]. The method has high-positioning accuracy and strong anti-interference ability, but it will pose a threat to human health and the ecological environment.

The technology of "accurate positioning" is generally used only when the robot has a jamming accident. The complexity and diversity of pipeline engineering promote the development of pipeline robot technology towards "autonomous movement," "internal and external communication," and "measurable position," so as to expand its application scope and reduce the risk of pipeline operation. In the process of cleaning, flaw detection, and other procedures of the pipeline robot, when it detects the pipe wall defect or its system failure, the staff outside the pipe needs to know its accurate position in the pipe in time, so as to quickly and accurately troubleshoot and resume operations. Therefore, the realization of wireless, reliable, and real-time "tracking" of pipeline robots has become one of the essential topics to improve the operating performance and practical value of pipeline robots. In theory, both the magnetic method and the pressure method can achieve the "tracking" function. In recent years, the tracking and positioning technology based on optical fiber vibration has also attracted the attention of researchers [11]. The technology needs to lay an optical fiber simultaneously as the pipeline, which will significantly increase the cost and limit the engineering test. Signal processing methods and vibration interference problems still need further research. In summary, the current various real-time tracking and positioning technologies have issues that need to be solved, such as reducing errors, operability, and cost issues. Further research is required at the basic theoretical and application levels.

To meet the requirement of real-time tracking and positioning, this paper presents a design scheme of the wireless tracking and positioning system for pipeline robots based on the ELF electromagnetic method using UAV, establishes the distribution model of ELF electromagnetic field in a complex pipeline environment, studies the propagation and attenuation characteristics of ELF electromagnetic wave through numerical and simulation analysis methods, and discusses the tracing algorithm of robot under the two conditions of horizontal-laying pipeline and inclined-laying pipeline, which lays a theoretical foundation for future practical application of the system.

2. Pipeline Robot Tracing and Positioning System Using UAV

The tracking and positioning technology studied in this paper includes two aspects: monitoring real-time motion state of the robot and indicating its precise position. To achieve the goal, ELF electromagnetic method with strong penetrating power for metal pipe wall and soil is a better choice. Still, traditional technology requires technicians to follow the pipeline trend for inspection. When the surface of the pipeline section is a harsh geographical environment such as rivers, lakes, alpine jungles, marshes, and gorges, it will bring great difficulties to the tracking and positioning. In order to design a system that does not require personnel tracking and can accurately grasp the real-time position information of the robot, this paper introduces the UAV technology, which has recently become a research hotspot. By exploiting its advantages such as flexibility, wide inspection range, and timely information transmission to the full, the pipeline robot can be tracked and positioned in real time, accurately and quickly.

The wireless tracking and positioning system of the pipeline robot using UAV is shown in Figure 1. Its working principle is as follows: an ELF electromagnetic wave transmitter is installed on the pipeline robot, and the periodic emission of ELF electromagnetic pulse is realized by transmitting antenna (solenoid coil); the time-varying ELF electromagnetic

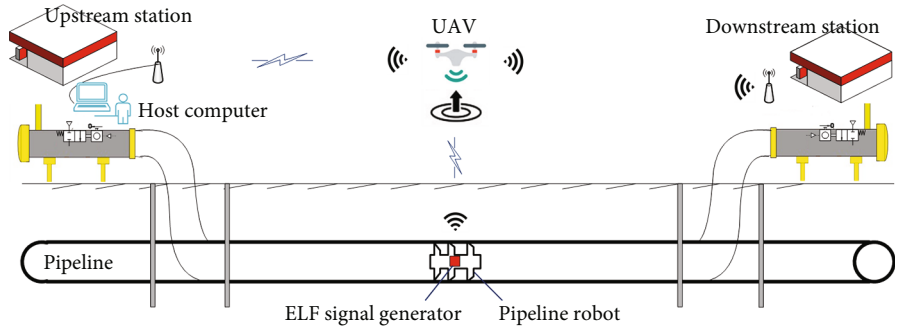

Figure 1: Wireless tracing and positioning system of pipeline robot using UAV.

field is established in the buried pipeline-ground environment by the strong penetrability of ELF wave; the receiving antenna (solenoid coil) carried by the tracking UAV converts the electromagnetic signal penetrating the metal pipe wall, overlying soil and air into voltage signal. After amplification and filtering, the electromagnetic field intensity is measured, and the location of ELF electromagnetic wave emitter is determined, and then the robot's position is determined.

When the pipeline robot gets stuck, the UAV can quickly find and approach the accident point according to the ELF electromagnetic field signal detected and report the location and environment of the accident to the operators at the upstream and downstream stations through the airborne wireless communication system. The operators can rapidly formulate the accident treatment plan based on the location, environmental photos of the incident site, and other information received and take timely actions, which significantly saves staffing and time. If the conditions permit, the UAV can work in tracking mode. The airborne-receiving device detects the ELF electromagnetic field signal in real-time, sets the parameters of flight control system according to the solution result to maintain the synchronization of flight tracking path and the robot, and simultaneously reports the information such as path and speed to operators through wireless communication, so that operators can keep track of the movement status of drone and pipeline robot. In the tracking process, if the abnormal motion status of the robot is found, such as moving more slowly, etc., the alarm can be sent out to remind the operator to make an emergency action plan in time.

The hardware part of the system can be realized by installing ELF signal transmitting on UAV and receiving modules on existing robots. The UAV equipped with a receiver to track and locate the robot can be flexibly selected by carrying a receiving module according to the working environment and conditions such as monitoring distance and flight environment, without developing a unique UAV system, which will significantly reduce the initial cost of the system. At the same time, the system can select the accident location positioning or real-time tracking according to the operation purpose. Based on experience, the robot does not need to work every time for real-time tracking, more importantly, in the event of a robot failure or found abnormal pipeline can accurately obtain its position information. Compared with the current precise positioning method, the drone can find the target more quickly and accurately. The operation range is incomparable to other methods, and the total operation cost is lower. Currently, the latest optical fiber early warning system also has high-positioning accuracy, extensive monitoring range, and low-operating cost, but the initial cost is enormous. It needs to lay a fiber with the pipeline at the same time and needs to build a distributed optical fiber-sensing system [12]. Especially for buried pipelines that have already been laid, reexcavation to lay the fiber is not the best option at extra cost. Therefore, considering the positioning effect, application difficulty, and economic factors, the pipeline robot tracking and positioning system based on UAV has unique advantages.

According to the working principle of the system, it can be seen that establishing the mathematical model of ELF electromagnetic field in pipeline environment and analyzing its distribution and attenuation characteristics are the theoretical basis for studying the position relation between the signal received by UAV (receiving coil) and pipeline robot (transmitting coil) to realize tracking and positioning, as well as the basis for the development algorithm of the application software of the tracking and positioning system.

3. Distribution Model of the ELF Magnetic Field in the Buried Pipe-Ground Environment

3.1. Establishment of Electromagnetic Field Distribution Model. The environment geometry of the tracking and positioning system is shown in Figure 2. M_1 in the pipeline is the transmission medium (oil or natural gas), pipe wall M_2 is the ferromagnetic material, M_3 is the overlying soil above the pipeline, M_4 is the air layer, and the anticorrosion insulation layer is ignored. The electromagnetic parameters of each layer are $\{\varepsilon_i, \mu_i, \sigma_i\}$ $(i = 1, 2, 3, \text{and } 4)$, ε_i is the permittivity, μ_i is the permeability, σ_i is the conductivity, and assuming that each layer is homogeneous and isotropic. The inner diameter of the buried pipeline is r_1, the external diameter is r_2, the distance between the surface and pipeline axis is r_3, and the thickness of the buried medium (overlying soil) is $h = r_3 - r_2$. The transmitting solenoid coil S on the robot is placed on the central axis of the pipeline by default, the distance from the surface is r_3; its radius a is far less than the distance between the transmitting coil and the receiving coil and

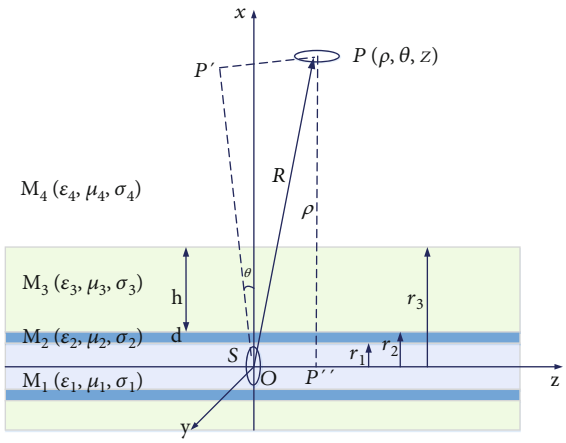

FIGURE 2: The environment geometry of the tracking and positioning system.

far less than the length of the transmitting coil 2 l; the number of coil turns is N, and the number of turns in unit length is n; the exciting current is $I = I_0 e^{-j\omega t}$, where ω is the current angular frequency. The cylindrical-coordinate system is established with the coil center as the origin, and the Z axis is on the central axis of the pipeline. The coordinate of the receiving coil on the UAV is $P(\rho, \theta, z)$, the space vector from the transmitting coil center to the receiving coil is $R = re_r$, and the distance is $r = (\rho^2 + z^2)^{1/2}$. The magnetic field distribution generated by the transmitting coil is axisymmetric.

The electric field intensity in the four-layer medium is E_1, E_2, E_3, and E_4, and the magnetic field intensity is H_1, H_2, H_3, and H_4, respectively. Due to the different properties of the two media, the field quantities varies at the interface. Knowing from the electromagnetic theory, the tangential and normal components of electric field E, D and H, B of magnetic field are continuous at the interface of transmission medium-pipe wall, pipe wall-overlying soil, and overlying soil-air in the cylindrical-coordinate system. When the transmitting solenoid coil is placed horizontally along the axis of the pipe, for the axisymmetric medium environment, the electric field intensity has only E_θ component, while the magnetic field intensity has H_ρ and H_z components. According to the Helmholtz equation, the expression of electric field intensity in each layer can be obtained by using the method of separation of variables as follows:

$$
\begin{aligned}
E_{1\theta}(\rho, z) &= -\frac{j\omega\mu_1 M}{2\pi^2}\int_0^\infty [A_1(\lambda)J_1(\rho x_1) + x_1 Y_1(\rho x_1)]\cos(\lambda z)d\lambda,\\
E_{2\theta}(\rho, z) &= -\frac{j\omega\mu_2 M}{2\pi^2}\int_0^\infty [A_2(\lambda)J_1(\rho x_2) + B_2(\lambda)Y_1(\rho x_2)]\cos(\lambda z)d\lambda,\\
E_{3\theta}(\rho, z) &= -\frac{j\omega\mu_3 M}{2\pi^2}\int_0^\infty [A_3(\lambda)J_1(\rho x_3) + B_3(\lambda)Y_1(\rho x_3)]\cos(\lambda z)d\lambda,\\
E_{4\theta}(\rho, z) &= -\frac{j\omega\mu_4 M}{2\pi^2}\int_0^\infty B_4(\lambda)Y_1(\rho x_4)\cos(\lambda z)d\lambda.
\end{aligned}
\tag{1}
$$

From $H = 1/j\omega\mu\nabla\times E$, the expression of magnetic field intensity in each layer can be obtained as follows:

$$
H = e_\rho\left(-\frac{1}{j\omega\mu}\frac{\partial E_\theta}{\partial z}\right) + e_z\left[\frac{1}{j\omega\mu}\left(\frac{E_\theta}{\rho} + \frac{\partial E_\theta}{\partial \rho}\right)\right]. \tag{2}
$$

The mathematical model of ELF electromagnetic field distribution under buried pipeline environment is obtained by expanding the expression as follows:

$$
\begin{aligned}
H_{1\rho}(\rho, z) &= -\frac{M}{2\pi^2}\int_0^\infty \lambda[A_1(\lambda)J_1(\rho x_1) + x_1 Y_1(\rho x_1)]\sin(\lambda z)d\lambda,\\
H_{1z}(\rho, z) &= -\frac{M}{2\pi^2}\int_0^\infty x_1[-A_1(\lambda)J_0(\rho x_1) + x_1 Y_0(\rho x_1)]\cos(\lambda z)d\lambda,\\
H_{2\rho}(\rho, z) &= -\frac{M}{2\pi^2}\int_0^\infty \lambda[A_2(\lambda)J_1(\rho x_2) + B_2(\lambda)Y_1(\rho x_2)]\sin(\lambda z)d\lambda,\\
H_{2z}(\rho, z) &= -\frac{M}{2\pi^2}\int_0^\infty x_2[-A_2(\lambda)J_0(\rho x_2) + B_2(\lambda)Y_0(\rho x_2)]\cos(\lambda z)d\lambda,\\
H_{3\rho}(\rho, z) &= -\frac{M}{2\pi^2}\int_0^\infty \lambda[A(\lambda)J_1(\rho x_3) + B_3(\lambda)Y_1(\rho x_3)]\sin(\lambda z)d\lambda,\\
H_{3z}(\rho, z) &= -\frac{M}{2\pi^2}\int_0^\infty x_3[-A_3(\lambda)J_0(\rho x_3) + B_3(\lambda)Y_0(\rho x_3)]\cos(\lambda z)d\lambda,\\
H_{4\rho}(\rho, z) &= -\frac{M}{2\pi^2}\int_0^\infty \lambda B_4(\lambda)Y_1(\rho x_4)\sin(\lambda z)d\lambda,\\
H_{4z}(\rho, z) &= -\frac{M}{2\pi^2}\int_0^\infty x_4 B_4(\lambda)Y_0(\rho x_4)\cos(\lambda z)d\lambda,
\end{aligned}
\tag{3}
$$

where $M = \pi a^2 NI$ is the magnetic moment of the transmitting solenoid coil, λ is an arbitrary real variable, J_0 and J_1 are the first kinds of modified Bessel functions, Y_0 and Y_1 are the second kinds of modified Bessel functions, and A_i and B_i are the undetermined coefficients which are derived from initial excitation conditions and boundary conditions, $x_i = [\lambda^2 - (\omega^2\mu_i\varepsilon_i + j\omega\mu_i\sigma_i)^2]^{1/2}$.

Therefore, when the receiving coil $P(\rho, \theta, z)$ in the UAV is placed vertically (the transmitting coil is parallel to the pipe axis and the receiving coil is perpendicular to the transmitting coil, as shown in Figure 3(a)), the magnetic field component of the ρ direction is mainly received, and the induced electromotive force obtained is as follows:

$$
\varepsilon_v(\rho, \theta, z) = -\frac{\partial \Phi_V}{\partial t} = -\frac{j\omega\mu_4 MA\cos\theta_v}{2\pi^2}\int_0^\infty x_4 B_4(\lambda)Y_0(\rho x_4)\cos(\lambda z)d\lambda. \tag{4}
$$

When the receiving coil $P(\rho, \theta, z)$ in the UAV is placed horizontally (the transmitting coil is parallel to the pipe axis, and the receiving coil is parallel to the transmitting coil, as shown in Figure 3(b)), the magnetic field component of the z direction is mainly received, and the induced

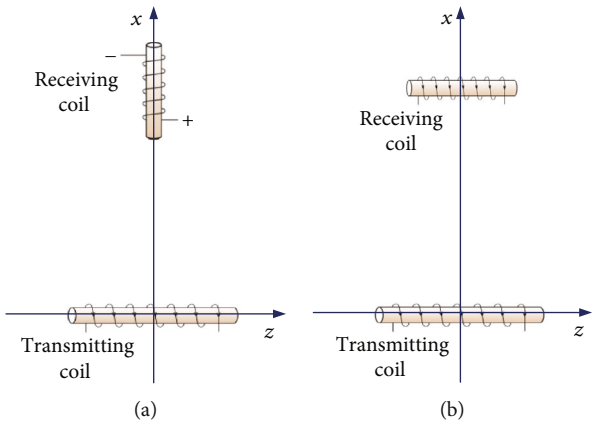

Figure 3: Coil relative position diagram.

electromotive force obtained is as follows:

$$\varepsilon_h(\rho,\theta,z) = -\frac{\partial \Phi_H}{\partial t} = -\frac{j\omega\mu_4 MA\cos\theta_h}{2\pi^2}\int_0^\infty \lambda B_4(\lambda)Y_1(\rho x_4)\sin(\lambda z)d\lambda, \tag{5}$$

where A is the cross-sectional area of the receiving coil, θ_v is the angle between the cross-sectional normal and the pipeline axial direction when the receiving coil is placed vertically on the ground, and θ_h is the angle between the cross-sectional normal and the pipeline radial direction when the receiving coil is placed horizontally.

3.2. Dipole Equivalent Magnetic Model. It can be seen from the above derivation process that the inversion method of transmitting source position by using the precise model to calculate the electromagnetic distribution at a certain point provides a theoretical basis for the subsequent research. Still, the computational process is too complex and not conducive to real-time analysis. Therefore, it is necessary to seek an equivalent model for analysis and calculation.

When the geometrical size of the transmitting coil (solenoid) is much smaller than the detection range, the length of the solenoid is much larger than the radius of the solenoid, and the excitation magnetic field is ELF field (or quasistatic field); the electromagnetic field generated by the excitation source can be equivalent to that generated by a magnetic dipole composed of a pair of point magnetic charges $\pm q_m$ with equal quantity and opposite sign [13].

Bessel function in the precise model, Formula (3) is written in power series first, and the expression is expanded by Bessel integral formula. Under the far-field condition, i.e., $(\rho, z) \gg (a, l)$, the series expression converges rapidly, so only the $n = 0$ term is needed in the series expressions of radial and axial magnetic field intensity, which is the precondition of using the equivalent magnetic dipole model. When $n = 0$, the radial and axial components of the magnetic induction intensity at the receiving coil $P(\rho, \theta, z)$ can be deduced as follows:

$$B_\rho(\rho,z) = \frac{n\mu_0 Ia^2\rho}{4}\left[\frac{1}{(r^2-2lz)^{3/2}} - \frac{1}{(r^2+2lz)^{3/2}}\right] = \frac{\mu_0 m}{4\pi r^5}\bullet 3\rho z,$$

$$\begin{aligned} B_z(\rho,z) &= \frac{n\mu_0 Ia^2}{4}\left[\frac{z-l}{(r^2-2lz)^{3/2}} - \frac{z+l}{(r^2+2lz)^{3/2}}\right] \\ &= \frac{n\mu_0 Ia^2}{4r^3}\left[\frac{2l}{r^2}\left(2z^2-\rho^2\right)\right] = \frac{\mu_0 m}{4\pi r^5}\bullet\left(2z^2-\rho^2\right), \end{aligned} \tag{6}$$

i.e.,

$$B_s = Be_r = \left(B_\rho{}^2 + B_z{}^2\right)^{1/2} e_r = \frac{\mu_0}{4\pi r^5}\left[3(m\bullet R)R - r^5 m\right], \tag{7}$$

where $m = 2ln\pi a^2 I$ is the magnetic moment of the transmitting solenoid coil.

The Formula (7) is precisely an expression of the magnetic field generated by a magnetic dipole with the magnetic moment $m = e_z m$ in cylindrical-coordinate system. It shows that it is theoretically feasible to use the equivalent magnetic dipole model when calculating the magnetic field in the far-field region.

According to $H_\rho(\rho, z)$, $H_z(\rho, z)$ obtained above, numerical simulation of spatial magnetic field distribution is carried out in the X-o-Z plane. The selected parameters are as follows: $n = 10$ turns/mm, $l = 500$ mm, $a = 50$ mm, $I = 0.3\sin(46\pi t)$A, taking the free space permeability $\mu_0 = 4\pi \times 10^{-7}$. When the receiving coil is $\rho = 8$ m away from the pipeline axis, the variation curve of the amplitude $|H|$ of the magnetic field intensity component with z is shown in Figure 4.

It can be seen from Figure 4(a) that the component H_ρ of the spatial magnetic induction intensity in the ρ direction generated by the equivalent magnetic dipole model presents a double-peak symmetric distribution in the axial direction of the pipeline. Near the center of the transmitting coil, the component of magnetic induction intensity in the ρ direction is the global minimum value; as the distance from the central point increases, the element of the magnetic induction intensity in this direction also increases, and two maximum signals can be detected at the front and rear positions of the transmitting coil. That is, in the case of single-coil reception, when the receiving coil moves directly above the transmitting coil, the detected signal is the weakest; when the receiving coil moves away from the transmitting coil, the detected signal is strengthened accordingly, which is the theoretical basis of positioning the pipeline robot with ELF electromagnetic wave. It can be seen from Figure 4(b) that the component H_z of magnetic induction intensity in the z direction presents a main-peak symmetric distribution and has a global maximum value near the center of the transmitting coil; that is, a global maximum signal can be measured in the z direction when the receiving coil is directly above the transmitting antenna, and there are two local maximum signals at the front and rear positions of the transmitting coil. The depth information of the transmitting coil can be obtained by measuring the amplitude width of the global maximum signal.

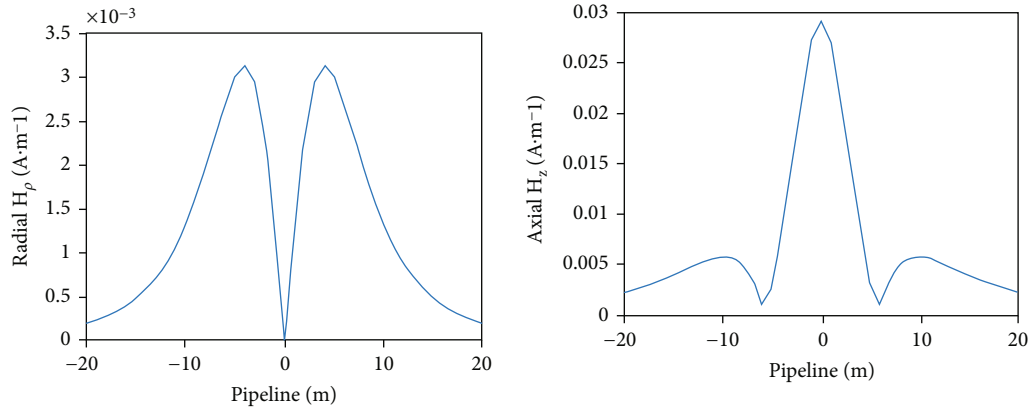

(a) Radial direction (b) Axial direction

FIGURE 4: Variation of magnetic field intensity $|H|$ with z.

4. ELF Electromagnetic Wave Attenuation Model

ELF electromagnetic field propagates outward in the form of wave. When ELF electromagnetic wave passes through conducting medium, part of it is absorbed by the medium, which causes electromagnetic wave attenuation, and part of it is consumed in the form of heat. In this section, the attenuation model of ELF electromagnetic wave in the buried pipe environment is derived using the equivalent magnetic dipole model.

The expression of the ELF magnetic field intensity in lossy medium can be obtained from the equivalent dipole model according to the wave equation

$$H_r = H_s e^{-\alpha d} e^{-j\beta d} = \frac{B_s}{\mu_0} e^{-\alpha d} e^{-j\beta d}, \tag{8}$$

where α is the attenuation constant, indicating the attenuation of the amplitude of the wave per unit length in the direction of propagation, and β is the phase-shift constant, meaning the change of the wave's phase per unit length in the direction of propagation.

$$\alpha = \omega \left\{ \frac{\mu\varepsilon'}{2} \left[\sqrt{1 + \left(\frac{\varepsilon''}{\varepsilon'} \right)^2} - 1 \right] \right\}^{1/2},$$
$$\beta = \omega \left\{ \frac{\mu\varepsilon'}{2} \left[\sqrt{1 + \left(\frac{\varepsilon''}{\varepsilon'} \right)^2} + 1 \right] \right\}^{1/2}, \tag{9}$$

where $\varepsilon' = \varepsilon$, $\varepsilon'' = \sigma/\omega$, and $\omega = 2\pi f$ are angular frequency, μ is magnetic permeability, ε is the dielectric constant of the medium, and σ is the electrical conductivity of the medium. The phase lag effect in low frequency electromagnetic wave transmission can be neglected, and the attenuation of amplitude is only needed care. The expression of α can be simplified for different mediums passing through the ELF electromagnetic wave propagation path.

In practice, if $\varepsilon''/\varepsilon' > 10^2$, the medium can be considered as a good conductor, such as pipe wall and overlying soil (especially for moist soil), and α can be approximated as

$$\alpha \approx \omega \sqrt{\frac{\mu\varepsilon''}{2}} = \sqrt{\frac{\omega\mu\sigma}{2}} = \sqrt{\pi f \mu \sigma}. \tag{10}$$

It can be seen from the Formula (10) that α increases with the increase of σ and transmitting frequency f. The ability of electromagnetic wave to penetrate the conductor is described by skin depth $\delta = 1/\alpha$; that is, the thickness of electromagnetic wave propagating when the amplitude of wave decreases to 0.37 times of the initial value. In order to penetrate the metal pipe wall, the thickness of the pipe wall must be guaranteed to be less than the skin depth. In order to penetrate the metal pipe wall, it must ensure that the wall thickness is less than the skin depth.

$$\mathrm{d} < \delta = \frac{1}{\alpha} = \frac{1}{\sqrt{\pi f \mu \sigma}}. \tag{11}$$

Therefore, $f < 1/(d^2 \pi \mu \sigma)$ indicates that increasing the skin depth by reducing the emission frequency can improve the penetration ability of electromagnetic waves.

If $\varepsilon''/\varepsilon' < 10^{-2}$, the medium can be considered as low-loss dielectrics, such as transmission fluid and air, and α can be approximated as

$$\alpha \approx \frac{\omega\varepsilon''}{2} \sqrt{\frac{\mu}{\varepsilon'}} = \frac{\sigma}{2} \sqrt{\frac{\mu}{\varepsilon}}. \tag{12}$$

In low-loss dielectric, β is the same as in the case of lossless, and α is independent of frequency. Then, in the buried pipeline environment, the pipe wall is regarded as a good conductor, and the transmission fluid, soil, and air are considered as low-loss dielectric. The expression of ELF electromagnetic wave from the transmitting coil to the receiving coil obtained by using the equivalent magnetic dipole model

Table 1: Electromagnetic constitutive parameters (low frequency and room temperature).

Medium	Relative permittivity (ε_r)	Conductivity (σ)	Relative permeability (μ_r)
Oil M1	2.1	$3 \times 10 - {}^{13}$	1
Gas M1	33.1	1×10^{-16}	1
Metal pipe (carbon steel) M2	∞	1×10^{7}	10-300
Overlying soil (moist) M3	16	1×10^{-2}	1
Air M4	1.0006	1×10^{-16}	1

Notes: $\varepsilon = \varepsilon_r \varepsilon_0$, $\varepsilon_0 = 8.854 \times 10^{-12}$F/m, $\mu = \mu_r \mu_0$, and $\mu_0 = 4\pi \times 10^{-7}$H/m.

Table 2: Transmitting antenna parameters.

Length (mm)	Coil radius (mm)	Coil turns (mm)	Excitation current (A)	Frequency (Hz)
500	50	20	0.3sin(50πt)A	10 ~ 100

Table 3: Environment parameters.

Internal diameter of the pipeline (mm)	Pipe thickness (mm)	Overlying soil thickness (m)	Elevation (m)
800	0 ~ 60	0 ~ 6	5

is as follows:

$$H_r = H_s e^{-\alpha d} e^{-j\beta d} = \frac{1}{4\pi r^5} \cdot \left[3(m \bullet R)R - r^2 m\right] e^{-r_1 \sigma_1 / 2\sqrt{\mu_1/\varepsilon_1}} e^{-\sqrt{\pi f \mu_2 \sigma_2} d} e^{-\sqrt{\pi f \mu_3 \sigma_3} h} e^{-(\rho - r_3)\sigma_3 / 2\sqrt{\mu_3/\varepsilon_3}}. \quad (13)$$

5. Analysis of the Influencing Factors of ELF Electromagnetic Field

Based on the above analysis, this section studies the effects of environmental parameters and working parameters on the ELF electromagnetic field intensity through numerical simulation. The research results will provide a theoretical basis for the selection of transmitter frequency, the optimization design of transmitting coil and receiving coil, the subsequent positioning algorithm research, and field experiments in the future.

In the buried pipeline environment, the electromagnetic constitutive parameters of each layer through which the electromagnetic wave passes are shown in Table 1. For both crude oil pipelines and gas pipelines, $e^{-r_1 \sigma_1 / 2\sqrt{\mu_1/\varepsilon_1}} \approx 1$ can be obtained by substituting the parameters in the table; that is, the medium in the pipeline will not cause the attenuation of electromagnetic wave. Similarly, for the air layer, $e^{-(\rho - r_3)\sigma_3 / 2\sqrt{\mu_3/\varepsilon_3}} \approx 1$; that is, the air layer will not cause the rapid attenuation too. Therefore, the following analysis mainly considers the influence of pipe wall and overlying soil layer on electromagnetic wave transmission. The selection of transmitting antenna and environment parameters is shown in Tables 2 and 3.

Without losing generality, the simulation calculation is carried out with the receiving antenna located directly above the transmitting antenna. The influence of different pipe thicknesses and overlying soil thicknesses on the received magnetic field intensity is analyzed, as shown in Figures 5 and 6.

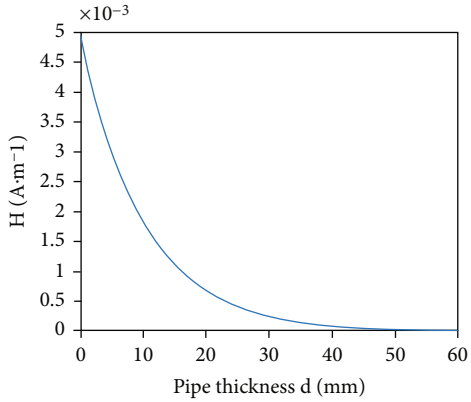

Figure 5: Effect of pipe thickness.

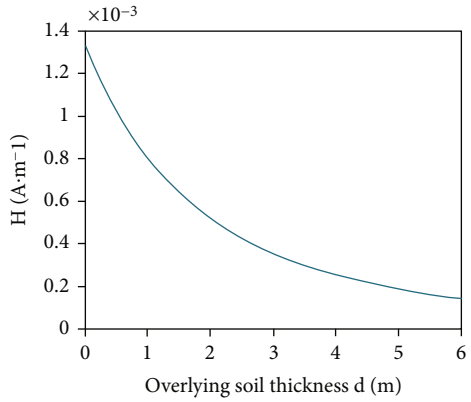

Figure 6: Effect of overlying soil thickness.

Figure 5 shows the exponential decay curve of the received magnetic field intensity with the increase of the pipe thickness when the transmitting frequency is 25 Hz and the overlying soil thickness is 2 m. Figure 6 shows the exponential decay curve of the received magnetic field intensity with the increase of overlying soil thickness when the transmitting frequency is 25 Hz and pipe thickness is 12 mm. It can be seen from the gradient of the two decay curves that the pipe thickness has a more significant attenuation on the magnetic field intensity. When designing the transmitting and receiving antenna, the influence of the pipe size and burial depth on the robot positioning should be fully considered.

Figure 7 shows the decay curve of the received magnetic field intensity with the increase of transmitting frequency when pipe thickness is 12 mm and overlying soil thickness is 3 m. The attenuation of the magnetic field intensity is more linear and smoother. However, the lower the frequency is not the better. For a transmitting antenna in a moving state, too low frequency will reduce the resolution of the receiving antenna signal processing. Figure 8 shows the exponential decay curves of the received magnetic field intensity with the increase of relative permeability and conductivity when the transmitting frequency is 25 Hz, pipe thickness is 12 mm, and overlying soil thickness is 3 m. The electromagnetic parameters, such as relative permeability and conductivity, are determined by the material properties of pipelines, including the carbon content and the doping of alloys. In addition, the variation characteristics of the surrounding conductivity and permeability of pipes with cathodic protection or corrosion need special attention.

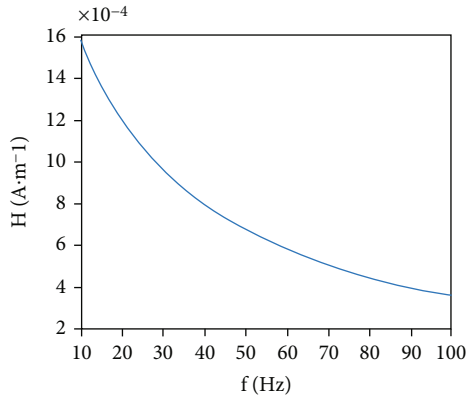

Figure 7: Effect of transmitting frequency.

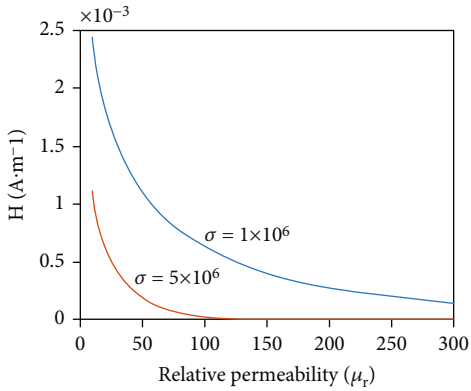

Figure 8: Effect of electromagnetic parameter.

6. Tracking and Positioning Method under Different Pipeline-Laying Conditions

The deduction and analysis are carried out when the transmitting antenna and the receiving antenna are perpendicular or parallel to each other and in the same plane. Still, in more general, the laying of buried or submarine pipelines is more complex and changeable. When the robot runs in the pipe, the axis direction of the transmitting coil can be approximately parallel to the axis direction of the pipeline, but the direction of the pipeline itself is constantly changing, so the relative position between the receiving antenna outside the pipeline (horizontal and vertical) and the transmitting coil is also changing, and the distribution law of the spatial magnetic field is also changing. Then, the positioning method of the pipeline robot is discussed in more general cases aiming at horizontal laying of pipelines and inclined laying of pipelines.

6.1. Horizontal Pipeline Environment. The distribution of the magnetic field in horizontal laying of pipeline is analyzed first. The axis of the transmitting solenoid coil is always parallel to the axis of pipeline by default; that is, the transmitting antenna is in the horizontal position. The receiving antenna is still in the vertical or horizontal direction to measure the horizontal and vertical components of magnetic field intensity, but it is not necessarily in the same plane as the transmitting antenna. The combination of horizontal transmission and vertical reception is shown in Figure 9. For the convenience of intuitive analysis, the output voltage of the receiver is directly used to represent the received magnetic field intensity, and the influence of the different relative positions on the voltage change is mainly discussed.

Based on the analysis of the ELF electromagnetic field distribution model, the components received in three directions (regardless of the position of the receiving antenna) can be obtained

$$\begin{aligned} H_x &= \frac{3M}{4\pi l^2 r}\sin^3\alpha\cos\alpha\cos^3\beta, \\ H_y &= -\frac{3M}{4\pi l^2 r}\sin^2\alpha\cos\alpha\sin\beta\cos^2\beta, \\ H_z &\frac{M}{4\pi l^2 r}\sin^2\alpha\cos^2\beta\left(3\cos^3\alpha - 1\right). \end{aligned} \tag{14}$$

The relationship between the output voltage of the sensor and the relative position of the transmitting antenna and the receiving antenna (represented by a, β, l, and r) is as follows:

$$U_v = CH_x = \frac{3CM}{4\pi l^2 r}\sin^3\alpha\cos\alpha\cos^3\beta, \tag{15}$$

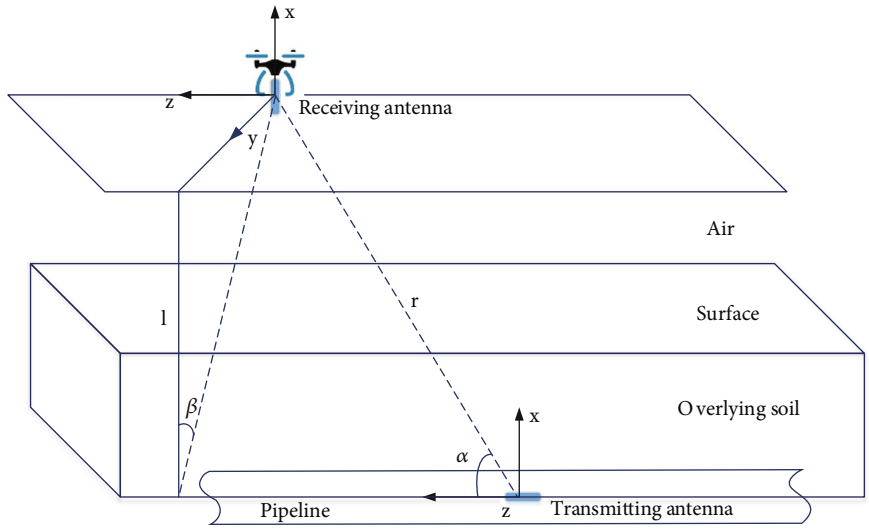

Figure 9: Horizontal transmission-vertical reception.

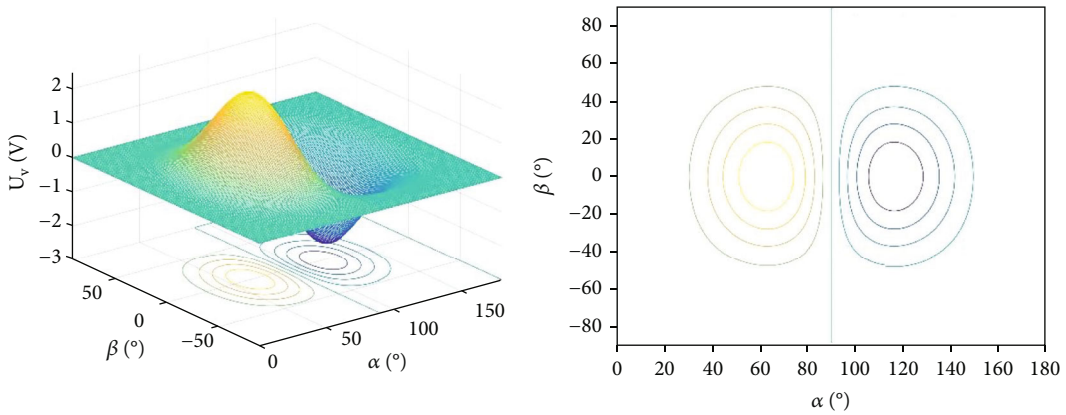

Figure 10: Distribution and plane isogram of U_v under horizontal transmission-vertical reception.

where C is the signal gain coefficient of the receiving sensor, and in this case, $C = 150$ V/T; M is the equivalent magnetic moment considering the attenuation caused by the pipe thickness and overlying soil, taking $M = 30\ \mathrm{A} \cdot \mathrm{m}^2$; $l = 5$ m, $\alpha \in [0, 180^\circ]$, and $\beta \in [-90\circ, 90\circ]$.

The distribution and plane isogram of U_v with the change of relative position under horizontal transmission-vertical reception is shown in Figure 10. It can be seen from the figure that the distribution of $|U_v|$ shows a double-peak characteristic, which is the same as the distribution feature on the X-o-Z plane obtained in the preceding. The UAV receives the electromagnetic field signal during the positioning process. According to the distribution regulation shown in the figure, UAV always travels along the gradient direction (the direction of the fastest descent or ascent of signal intensity) and explores the peak and trough positions shown in the figure. The midpoint of the peak and trough is the position directly above the robot. If the voltage is taken as an absolute value, the trough becomes a peak, and the robot is at the midpoint of the two peaks.

When the horizontal-receiving mode is adopted, the receiving antenna is parallel to the ground during the flight, but the course is not necessarily the same as the direction of the pipeline; that is, the axis of the receiving antenna and the axis of the transmitting antenna may produce a certain angle γ on the same horizontal plane. $\gamma = 0\circ$, the receiving antenna axis, is parallel to the transmitting antenna axis, and $\gamma = 90\circ$, the receiving antenna axis, is vertical to the transmitting antenna axis, as shown in Figure 11.

The output voltage of the sensor under this working condition is

$$U_h = CH_h = C\left(H_z \cos\gamma - H_y \sin\gamma\right) = \frac{3Cm}{4\pi l^2 r} \sin^2\alpha \cos^2\beta \cdot \left[\left(3\cos^3\alpha - 1\right)\cos\gamma - \cos\alpha \sin\beta \sin\gamma\right]. \tag{16}$$

The distribution and plane isogram of U_h with the change of relative position under horizontal transmission-horizontal

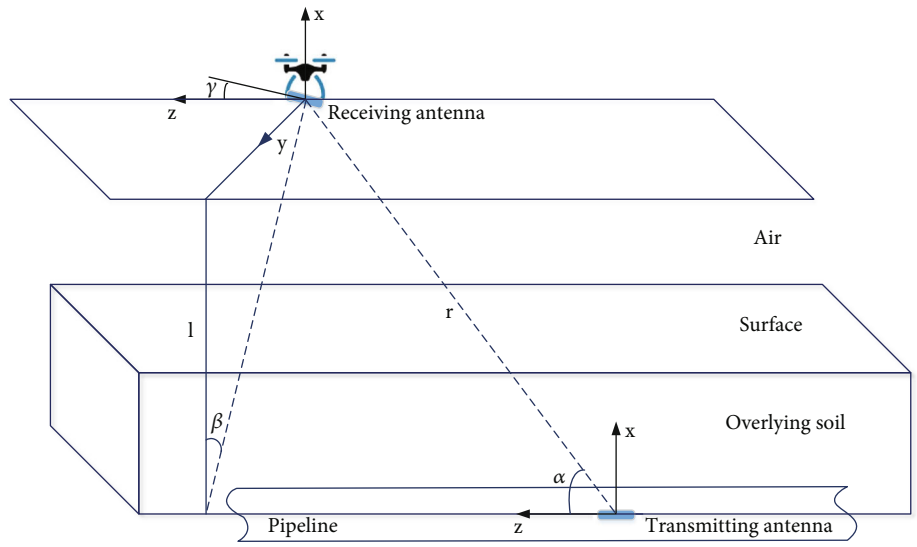

Figure 11: Horizontal transmission-horizontal reception.

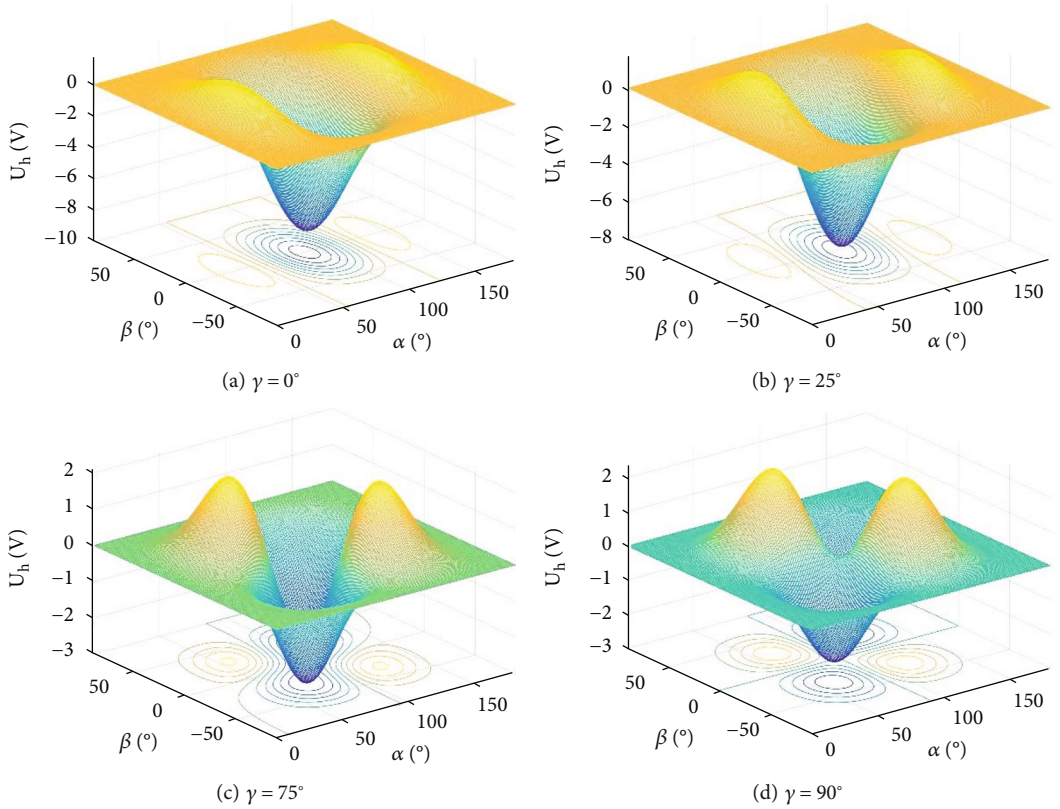

Figure 12: Distribution and plane isogram of U_h under horizontal transmission-horizontal reception.

reception is shown in Figure 12. When $\gamma = 0\circ$, it can be seen that the distribution of U_h has single peak and double troughs and the absolute output voltage has a global maximum value with two local maximum values on both sides of it, which is the same as the analysis conclusion on the two-dimensional plane. When tracking and positioning, the UAV searches for the global maximum value along the steepest ascent curve of the output voltage amplitude to locate the pipeline robot. When γ increases gradually, the contour deflects and the positions of local maximum values rotate. The troughs representing the global maximum gradually change from single trough to connected trough, and finally forms double troughs. When $\gamma = 90\circ$; that is, the axis of receiving antenna is perpendicular to the direction of the pipe; two global maximum values and two local maximum values are distributed at an equal interval of 45°. To sum up, the vertical reception should be used primarily in the positioning process by finding the midpoint of the peak and trough. Then, the horizontal reception is used

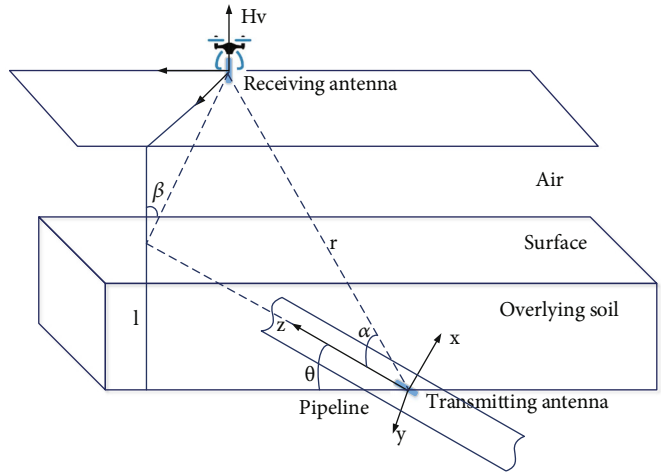

Figure 13: Inclined transmission-vertical reception.

as the supplement by searching for the maximum value of the sensor output signal to adjust the course of the UAV and assist the position verification.

6.2. Inclined Pipeline Environment. In the practical long-distance pipeline-laying process, affected by rugged terrain, obstacles, and other factors, it is difficult for the pipeline to keep parallel with the horizontal plane for a long distance, and there are a lot of slopes and corners. Therefore, it is necessary to study the electromagnetic field distribution characteristics in the case of the inclined pipeline. As shown in Figure 13, the angle between the pipeline and the horizontal plane (inclination angle) is θ, and $\theta \in [0^\circ \sim 90^\circ]$ has the following relationship:

$$\mathrm{r} = \frac{l}{\sin\theta\cos\alpha + \cos\theta\sin\alpha\cos\beta}. \tag{17}$$

The components received in three directions can be obtained

$$\begin{aligned} H_x &= \frac{3M}{4\pi l^3}\sin\alpha\cos\alpha\cos\beta(\sin\theta\cos\alpha + \cos\theta\sin\alpha\cos\beta)^3, \\ H_y &= \frac{3M}{4\pi l^3}\sin\alpha\cos\alpha\sin\beta(\sin\theta\cos\alpha + \cos\theta\sin\alpha\cos\beta)^3, \\ H_z &\frac{M}{4\pi l^3}\left(3\cos^2\alpha + 1\right)(\sin\theta\cos\alpha + \cos\theta\sin\alpha\cos\beta)^3. \end{aligned} \tag{18}$$

Considering the vertical-receiving mode shown in Figure 13, the vertical magnetic field intensity is as follows:

$$H_v = H_x\cos\theta + H_z\sin\theta. \tag{19}$$

The relationship between the output voltage of the sensor and the relative position of the pipeline-receiving antenna is as follows:

$$\begin{aligned} U_v = CH_v = \frac{CM}{4\pi l^3}&\left[\sin\theta\left(2\cos^2\alpha - \sin^2\alpha\right) + 3\cos\theta\sin\alpha\cos\alpha\cos\beta\right] \\ &\cdot(\sin\theta\cos\alpha + \cos\theta\sin\alpha\cos\beta)^3. \end{aligned} \tag{20}$$

The distribution and plane isogram of U_v with the change of relative position under inclined transmission-vertical reception is shown in Figure 14. It can be seen from the figure that when the gradient of pipeline is small, such as $\theta = 10$ degrees (see Figures 14(a) and 14(b)), the peak-trough characteristic is still apparent, and the pipeline robot can be located by finding the midpoint of the wave peak and trough; when the pipeline gradient increases gradually (see Figure 14(c)), the wave peak topples and falls to the side of the trough, and the trough rises gradually (corresponding amplitude gets gradually smaller); when $\theta > 60^\circ$ (see Figure 14(d)), the trough disappears and the peak appears only at the position where the receiver is far from the robot; and when $\theta > 80^\circ$ (Figure 14(e)), the wave peak and trough have disappeared, and it is not easy to locate the position of the robot. However, considering that the gradient of long-distance pipeline is generally not more than 45° in practice, ELF tracking and positioning method is still available.

When the receiving antenna is parallel to the ground, as shown in Figure 15, the angle between the axis of the receiving antenna and the axis of the transmitting is still γ. The magnetic field intensity in the horizontal direction is

$$H_h = H_z\cos\theta\cos\gamma - H_y\sin\gamma - H_x\sin\theta\cos\gamma. \tag{21}$$

The output voltage of the sensor under this working

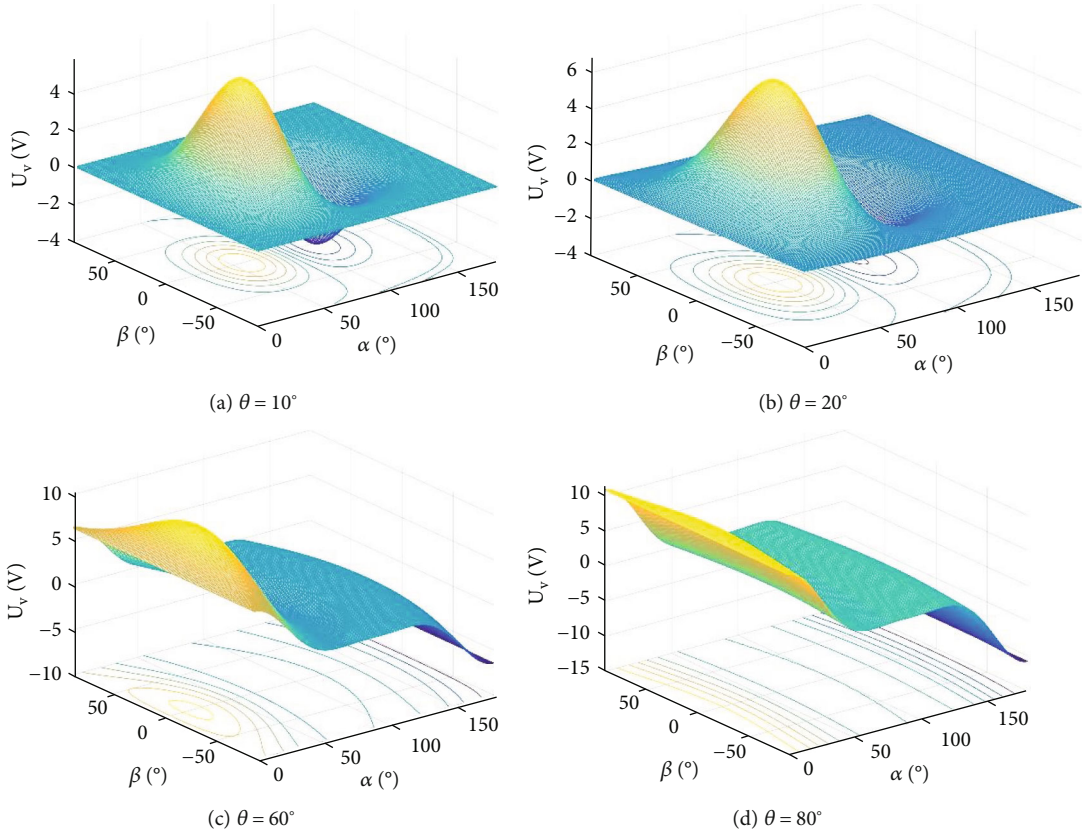

FIGURE 14: Distribution and plane isogram of U_v under inclined transmission-vertical reception.

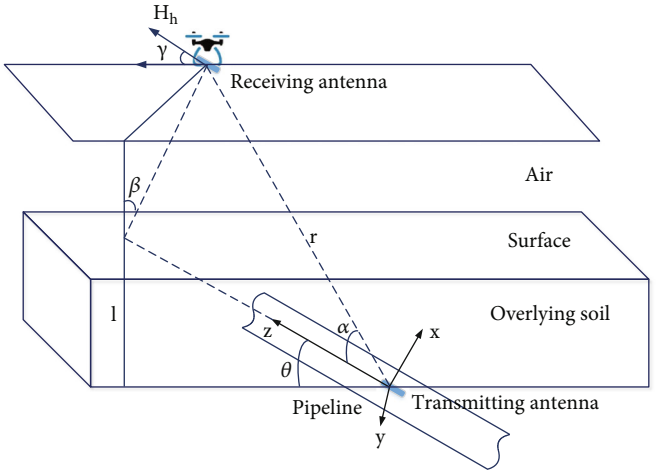

FIGURE 15: Inclined transmission-horizontal reception.

condition by substituting Formula (18) is

$$U_h = CH_h = \frac{CM}{4\pi l^3}\left[\cos\theta\left(2\cos^2\alpha - \sin^2\alpha\right)\cos\gamma - 3\cos\theta\sin\alpha\cos\alpha\cos\beta\cos\gamma + 3\sin\alpha\cos\alpha\cos\beta\sin\gamma\right](\sin\theta\cos\alpha + \cos\theta\sin\alpha\cos\beta)^3. \quad (22)$$

There are four variables α, β, γ, and θ in the above formula, so the distribution of U_h is complicated. Figure 16 shows the distribution and plane isogram of U_h when $\theta = 20\circ$, 40°, and 60° under $\gamma = 0\circ$, 30°, 60°, and 90°, respectively. It can be seen from the figure that when $\theta = 20\circ$ (see Figure 16(a)), the distribution of the global maximum (trough) and local maximum (peak) is pronounced. With the increase of γ, the positions of the two peaks are deflected, and the trough is gradually split into two troughs, and finally evolve into double peaks and double troughs. The robot is at the midpoint of the peak and trough, which can be used for positioning. When $\theta = 40\circ$ (see Figure 16(b)), there is only one global maximum value (single trough) under $\gamma = 0\circ$.

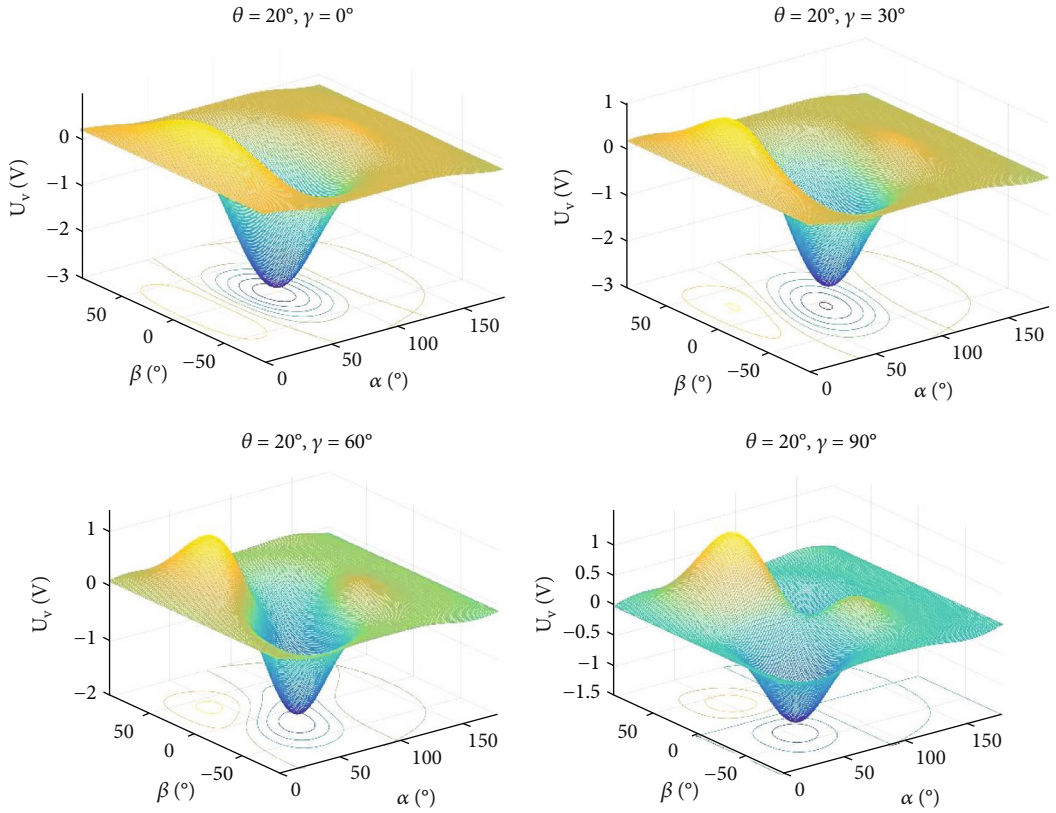

(a) $\theta = 20°$, $\gamma = 0°$, $30°$, $60°$, and $90°$

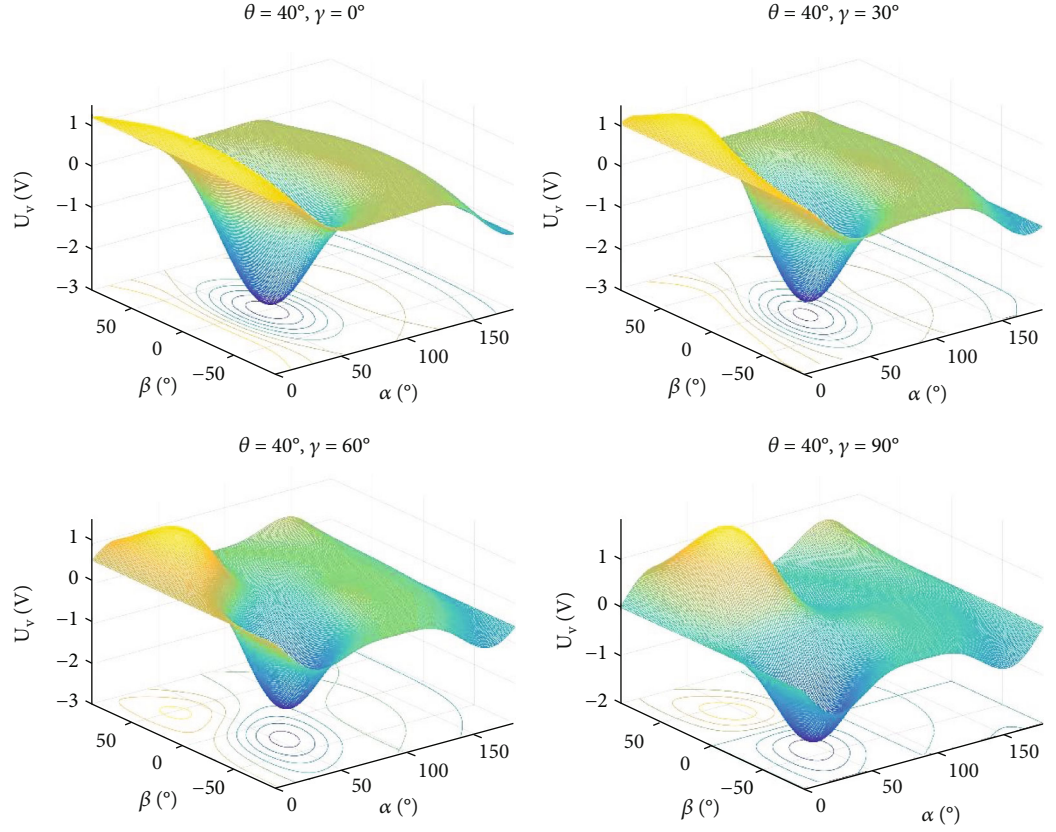

(b) $\theta = 40°$, $\gamma = 0°$, $30°$, $60°$, and $90°$

Figure 16: Continued.

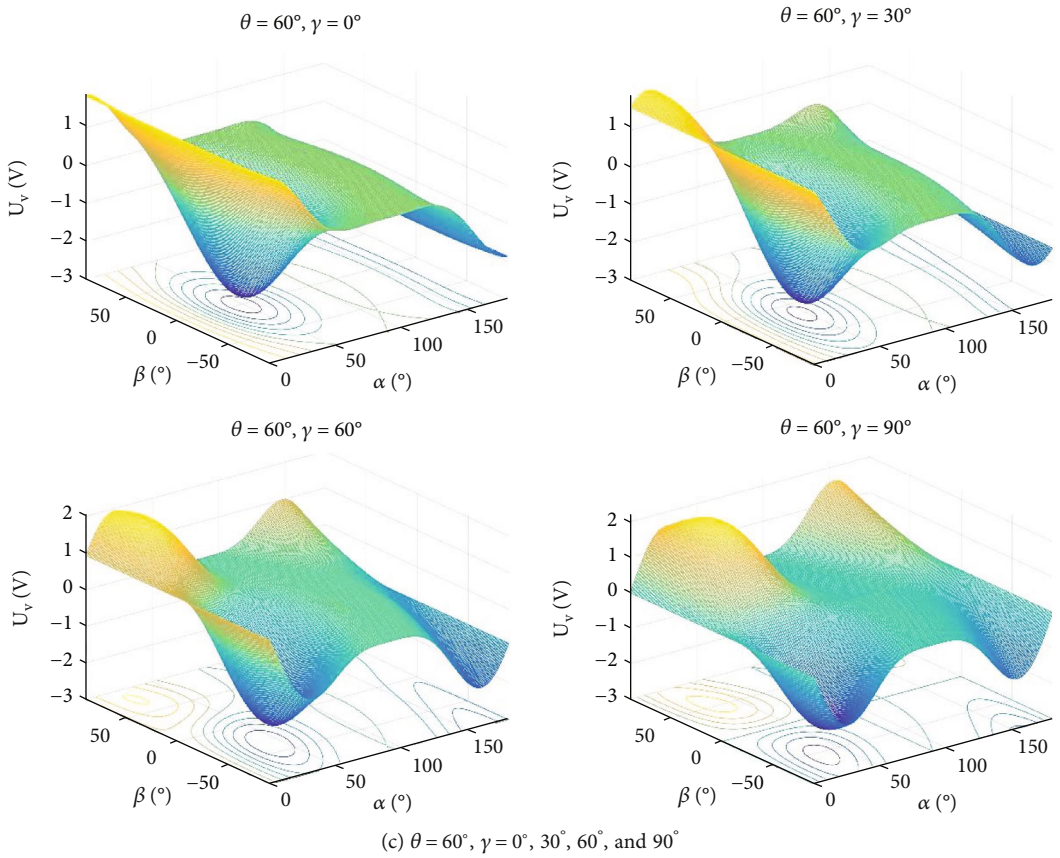

(c) $\theta = 60^{\circ}$, $\gamma = 0^{\circ}$, 30°, 60°, and 90°

Figure 16: Distribution and plane isogram of U_h under inclined transmission-horizontal reception.

The position of the trough deflects to the rear of the robot, and a local maximum (peak) is generated, which increases with γ. The axial position of the pipe can be judged by the midpoint of the wave and trough. Although the precise position of the robot cannot be located, it can be considered whether it is in front or rear of the UAV. When $\theta = 60\circ$ (see Figure 16(c)) and if γ is small, only the global maximum (single trough) can no longer locate the robot and the direction of the pipeline cannot be determined; if γ is further increased, a local maximum value (peak) appears, and the boundary line of the peak and valley is the pipe axis. Therefore, when the pipeline gradient is large, the horizontal-receiving antenna can hardly locate the pipeline robot. Still, it can help the UAV to return to the pipeline direction when it is yawing. At the same time, as mentioned above, the practical pipeline does not have such a large gradient.

7. Conclusion

The tracking and positioning of pipeline robot are closely related to the safe and reliable operation of pipeline cleaning and inspection equipment loaded by the robot. The tracking and positioning system using UAV presented in this paper is to improve the automation level and engineering applicability of pipeline robot and meet the urgent needs of trenchless detection and risk-elimination in pipeline engineering. The mathematical model of the ELF electromagnetic field distribution in the metal pipe environment established from classical electromagnetic theory provides a theoretical basis for the equivalent magnetic dipole model to describe the real system. The equivalent model is used to analyze the influence of electromagnetic parameters, geometrical dimensions, and transmitting frequency on the ELF electromagnetic field distribution characteristics in engineering pipeline environment. The investigation of ELF electromagnetic field distribution law under two conditions of laying pipeline horizontally and laying pipeline inclined is the prerequisite of realizing the accurate positioning of pipeline robot. The tracking method of moving robot inside the pipeline based on this research has the advantages of convenience, efficiency, and high accuracy, which not only ensures the safe operation of robot but also provides convenient conditions for pipeline construction operation such as excavation, maintenance, and robot's removal when blocking accidents occur. The tracking and positioning method is mainly studied by numerical analysis in this paper, and the engineering application of the technology will be discussed in-depth in the future.

Data Availability

The raw data used to support the findings of this study are included within the article.

Conflicts of Interest

The authors declared that they have no conflicts of interest regarding this work.

Acknowledgments

This research is supported by the Key Scientific Research Project of Colleges and Universities of Henan Province (Grant No. 23B440001) and the National Key Research and Development Program of China (Grant No. 2020YFB1712404).

References

[1] S. Roh and H. R. Choi, "Differential-drive in-pipe robot for moving inside urban gas pipelines," *IEEE Transactions on Robotics*, vol. 21, no. 1, pp. 1–17, 2005.

[2] J. Okamoto Jr., J. C. Adamowski, M. Tsuzuki, F. Buiochi, and C. S. Camerini, "Autonomous system for oil pipelines inspection," *Mechatronics*, vol. 9, no. 7, pp. 731–743, 1999.

[3] H. Ge, K. Li, L. Wang, S. Chen, Q. Xu, and Z. Li, "Status and prospect of pig tracking and positioning technology," *Pipeline Technique and Equipment*, vol. 3, pp. 1–7, 2022.

[4] H. Qiu, H. Wang, W. Sun, X. Zhao, B. Li, and C. Chen, "Present and future development of pig tracing and positioning techniques," *Oil & Gas Storage and Transportation*, vol. 34, no. 10, pp. 1033–1037, 2015.

[5] H. Qi, X. Zhang, H. Chen, and J. Ye, "Tracing and localization system for pipeline robot," *Mechatronics*, vol. 19, no. 1, pp. 76–84, 2009.

[6] H. Qi, J. Ye, X. Zhang, and H. Chen, "Wireless tracking and locating system for in-pipe robot," *Sensors and Actuators: A Physical*, vol. 159, no. 1, pp. 117–125, 2010.

[7] E. Paperno, I. Sasada, and E. Leonovich, "A new method for magnetic position and orientation tracking," *IEEE Transactions on Magnetics*, vol. 37, no. 4, pp. 1938–1940, 2001.

[8] J. Herbst, "Non-destructive testing of sewer pipes by an acoustical method," *IEEE Instrumentation & Measurement Technology Conference*, vol. 1, pp. 849–853, 2002.

[9] R. Murayama, S. Makiyama, M. Kodama, and Y. Taniguchi, "Development of an ultrasonic inspection robot using an electromagnetic acoustic transducer for a lamb wave and an SH-plate wave," *Ultrasonics*, vol. 42, no. 1-9, pp. 825–829, 2004.

[10] X. Zhang, J. Li, and H. Chen, "Visual feature recognition of an X-ray based inspection pipeline robot," *International Conference on Control and Automation*, vol. 2, pp. 966–970, 2005.

[11] W. Gou, L. Zhang, and G. Li, "Application of fiber pre-warning system in monitoring trajectory of pig," *Automation in Petro-Chemical Industry*, vol. 55, no. 3, pp. 80–82, 2019.

[12] Q. Hongquan, Z. Tong, B. Fukun, and P. Liping, "Vibration detection method for optical fibre pre-warning system," *IET Signal Processing*, vol. 10, no. 6, pp. 692–698, 2016.

[13] E. Paperno and A. Plotkin, "Cylindrical induction coil to accurately imitate the ideal magnetic dipole," *Sensors and Actuators A: Physical*, vol. 112, no. 2-3, pp. 248–252, 2004.